DUAL-BAND MODIFIED WILKINSON POWER DIVIDER WITHOUT TRANSMISSION LINE STUBS AND REACTIVE COMPONENTS

Y. Wu, Y. Liu, and S. Li

School of Electronic Engineering
Beijing University of Posts and Telecommunications
China

Abstract—In this paper, a novel modified Wilkinson power divider without transmission line stubs (such as short-circuit stubs and open-circuit stubs) and reactive components (such as isolation inductor L and capacitor C) is developed for dual-band applications. This symmetric power divider consists of six sections of transmission lines and an isolation resistor, and the corresponding nonlinear design equations are derived by using the even- and odd-mode analysis. Moreover, by solving the final nonlinear design equations, accurate numerical design data along with different frequency ratios are obtained, and the effective normalized parameters are given simultaneously in the figure and table formats for specific applications. To theoretically verify the design parameters, an ideal equal power divider operating at both 900 MHz and 5.85 GHz is simulated. Finally, the proposed structure and design method are validated by simulated and experimental results of a typical microstrip planar power divider operating at both 1 GHz and 3.5 GHz.

1. INTRODUCTION

Power dividers and combiners, known as famous three-port devices, are very important for microwave and millimeter-wave systems, because they can be widely used in balanced power amplifier, antenna feed networks, measurement systems etc. Recently, due to the requirement of dual-band microwave or wireless communication systems (such as GSM, TD-SCDMA), the researches on dual-band impedances matching [1–3] and dual-band Wilkinson power dividers

---

Corresponding author: Y. Wu (wuyongle138@gmail.com).

including equal cases [4–12] and unequal cases [13–16] become very popular. In addition, it is obvious that traditional distributed-elements Wilkinson power divider [17] with quarter-wavelength transmission lines and unequal lumped-elements one [18] cannot satisfy the flexible dual-band applications. In various kinds of dual-band modified Wilkinson power dividers proposed in [4–12], in fact, the frequency characteristics including matching, isolation, and transmission are different according to different structures. For example, narrowband [5, 6] and broadband [7, 9] dual-band power dividers can be chosen in narrowband and broadband dual-band systems, respectively. Moreover, novel Wilkinson power dividers with harmonic suppression [19], size-reduction [20, 21] or high power-dividing ratios [22] are also researched; however, these new modified power dividers based on special technologies are beyond the need for dual-band microwave systems.

In this article, we propose a novel dual-band modified Wilkinson power divider without transmission line stubs and reactive components. This researched symmetric structure consisting of three groups (six sections) of transmission lines and an isolation resistor can satisfy flexible dual-band operations. The conventional even- and odd-mode analysis is applied to obtain the nonlinear design equations in theory. For convenience in designing various practical dual-band power dividers based on this proposed structure, the normalized characteristic impedances of transmission lines and resistance value of the isolation resistor are given in detail in this paper. In the stage of verifying the design theory of this proposed power divider, a simulated equal dual-band (The center frequencies are 900 MHz and 5.85 GHz) power divider is presented first. Then, a fabricated equal (-3 dB) microstrip power divider operating at both 1 GHz and 3.5 GHz, as a typical sample, certifies the proposed structure and the corresponding design method experimentally. Finally, good agreements are observed in both simulated and measured results. In summary, this proposed power divider has the following main features: 1) The enhanced bandwidth of each band can be achieved due to the lack of transmission line stubs as resonant structures [9]; 2) Since there are not any reactive components, this proposed dual-band modified power divider can be used at very high-frequencies, such as the operating frequency f which is greater than three; and 3) The range of frequency ratios is very wide, for example, the frequency ratios lie between 2.5 and 6.5 for common microstrip implementations. Therefore, this power divider can be applied in two high-separated bands (such as 1 GHz and 6 GHz) systems with wideband characteristics.

2. THE PROPOSED CIRCUIT STRUCTURE AND DESIGN EQUATIONS

Figure 1 shows the circuit structure of the proposed dual-band power divider. For convenience, the transmission line parameters shown in Fig. 1 such as characteristic impedances (z_1, z_2, z_3) and the isolation resistor (r) are normalized with the terminal characteristic impedance (Z_0). Thus, in practical circuit implementation, the final design parameters should be obtained according to special terminal characteristic impedance Z_0 (such as $50\,\Omega$). As shown in Fig. 1, two sections of transmission lines are inserted between the input port and the isolation resistor as main parts of dual-band impedance transformers. Two output ports are extended instead of adopting transmission line stubs or reactive components such as inductors L and capacitors C. Therefore, to guarantee that all ports are matched ideally and the isolation between P2 and P3 is perfect, it is usual to apply the conventional even- and odd-mode analysis. The simple equivalent circuit structures are presented in Fig. 2 and Fig. 3, respectively for the even- and odd-mode analysis.
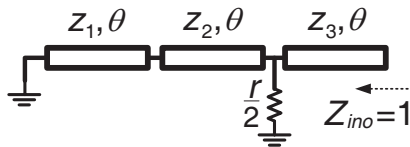
As depicted in Fig. 2, this dual-band impedance transformer includes three sections of transmission lines. Based on the transmission
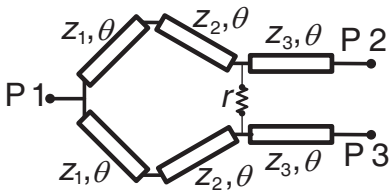
Figure 1. The circuit structure of the proposed dual-band power divider.
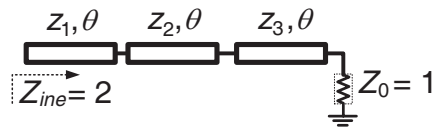
Figure 2. The equivalent circuit structure for the even-mode analysis.

Figure 3. The equivalent circuit structure for the odd-mode analysis.

line theory, we can obtain the following equations:

$$z_{in1} = z_3 \frac{1 + jz_3 \tan(\theta)}{z_3 + j1 \tan(\theta)}, \tag{1}$$

$$z_{in2} = z_2 \frac{z_{in1} + jz_2 \tan(\theta)}{z_2 + jz_{in1} \tan(\theta)}, \tag{2}$$

$$z_{ine} = z_1 \frac{z_{in2} + jz_1 \tan(\theta)}{z_1 + jz_{in2} \tan(\theta)} = 2. \tag{3}$$

By combining (1) and (2), we can also obtain

$$z_{in2} = \frac{z_2 z_3 - z_2^2 \tan^2(\theta) + jz_2 z_3 (z_2 + z_3) \tan(\theta)}{z_2 z_3 - z_3^2 \tan^2(\theta) + j \tan(\theta)(z_2 + z_3)}. \tag{4}$$

In addition, the Equation (3) is rewritten as

$$z_{in2} = z_1 \frac{2 - jz_1 \tan(\theta)}{z_1 - j2 \tan(\theta)}. \tag{5}$$

By combining (4) and (5) and separating the real and imaginary parts, the following equations can be obtained:

$$z_1 z_2 z_3 + \left[z_1^2 z_2 + z_1^2 z_3 + z_1 z_2^2 - 2z_1 z_3^2 - 2z_2 z_3 (z_2 + z_3) \right] \tan^2(\theta) = 0, \tag{6}$$

$$\tan(\theta) \left[z_1^2 z_3^2 \tan^2(\theta) - z_1^2 z_2 z_3 - z_1 z_2 z_3 (z_2 + z_3) \right.$$
$$\left. + 2z_1 (z_2 + z_3) + 2z_2 z_3 - 2z_2^2 \tan^2(\theta) \right] = 0. \tag{7}$$

From Fig. 3, the input impedance can be calculated by

$$z_{ino} = z_3 \frac{\frac{z_{in}r}{2z_{in}+r} + jz_3 \tan(\theta)}{z_3 + \frac{jz_{in}r \tan(\theta)}{2z_{in}+r}} = 1, \tag{8}$$

where

$$z_{in} = z_2 \frac{jz_1 \tan(\theta) + jz_2 \tan(\theta)}{z_2 + j \tan(\theta)[jz_1 \tan(\theta)]}. \tag{9}$$

Then, after separating the real and imaginary parts of (8) and (9), two independent equations can be expressed by

$$\begin{cases} \dfrac{z_2 z_3 (z_1 + z_2)(r - 2)}{z_2 - z_1 \tan^2(\theta)} + z_3^2 r = 0, \\[4mm] \dfrac{(r - 2z_3^2) z_2 (z_1 + z_2) \tan^2(\theta)}{z_2 - z_1 \tan^2(\theta)} = z_3 r. \end{cases} \tag{10}$$

According to Equations (6), (7), and (10), the final nonlinear design equations of normalized characteristic impedances and isolation resistance are simplified and summarized as follows,

$$z_1 z_2 z_3 + \left(z_1^2 z_3 + z_1^2 z_2 + z_2^2 z_1 - 2z_2^2 z_3 - 2z_3^2 z_2 - 2z_3^2 z_1\right)\tan^2(\theta) = 0, \quad (11)$$

$$2(z_1 z_2 + z_2 z_3 + z_1 z_3) - z_1 z_2 z_3 (z_1 + z_2 + z_3) + \left(z_1^2 z_3^2 - 2z_2^2\right)\tan^2(\theta) = 0, \quad (12)$$

$$z_2(1 - z_3^2)(z_1 + z_2)\tan^2(\theta) - z_3\left[z_2 - z_1\tan^2(\theta)\right]\left[1 + z_3^2\tan^2(\theta)\right] = 0, \quad (13)$$

$$r = \frac{2\left[1 + z_3^2\tan^2(\theta)\right]}{1 + \tan^2(\theta)}. \quad (14)$$

Obviously, there are four variables in the above four independent expressions when the electrical length θ is given. It can be observed that Equations (11)–(14) are even functions of $\tan(\theta)$, namely, the total nonlinear equations will be unchanged while the absolute value of $\tan(\theta)$ is fixed. Furthermore, the electrical length θ depends on the operating frequency. Here, assume that the center frequencies of arbitrary dual-band are f_1 and $f_2 = pf_1$, where p is the frequency ratio and $p \geq 1$. Therefore, the corresponding electrical lengths θ_{f_1} and θ_{f_2} satisfy the relationship as follows,

$$\theta_{f_2} = p\theta_{f_1}. \quad (15)$$

To ensure that the absolute values of $\tan(\theta_{f_1})$ and $\tan(\theta_{f_2})$ are constant, we can finally obtain the following solutions

$$\tan(\theta_{f_2}) = \pm\tan(\theta_{f_1}). \quad (16)$$

Thus, under the conditions (15) and (16), the final positive electrical length θ_{f_1} can be derived directly as

$$\theta_{f_1} = \frac{n\pi}{p \pm 1}, \ n \in \{1, 2, 3, \dots\}. \quad (17)$$

In practical circuit implementations, compact structure is preferable. According to (17), the positive and theoretical minimum of electrical length is chosen as

$$\theta_{f_1} = \frac{\pi}{1 + p}. \quad (18)$$

Note that the design Equation (18) for compact structures is only chosen to be discussed in the following sections. Based on nonlinear Equations (11)–(14) and (18), the closed-form design equations cannot be derived analytically. However, for this kind of proposed power divider, the normalized design parameters may be easily obtained through numerical optimization method instead of closed-form design equations. Therefore, the normalized design parameters illustrated in the next section would be useful for future applications.

3. NORMALIZED DESIGN PARAMETERS CHART AND DATA

By solving Equations (11)–(14) numerically, the results of normalized characteristic impedances (z_1, z_2, z_3) and isolation resistance (r) varying with frequency ratio p are shown in Fig. 4. As depicted in Fig. 4, the power divider can operate at the frequency ratio ranging from 2.5 to 6.5, with characteristic impedances in the range of from 0.5143 to 2.9769 (These characteristic impedances can satisfy common microstrip applications). The maximum normalized value of the isolation resistor (r) in Fig. 4 is 4.9509 for $p = 2.5$. Therefore, this proposed power divider is very suitable for two high-separated bands systems. Furthermore, the accurate normalized parameters with typical frequency ratios are listed in Table 1 and Table 2 guaranteeing that future application repetition is convenient. Considering that (18) can be easily used to calculate the electrical length, its values are not

Table 1. Normalized design parameters with typical frequency ratios ($2.5 \leq p \leq 4.4$).

The Frequency Ratio	Characteristic Impedances			Isolation Resistance
p	z_1	z_2	z_3	r
2.5	2.7901	1.7744	1.8476	4.9509
2.6	2.1778	1.5333	1.4633	3.3393
2.7	1.8628	1.4429	1.2690	2.6879
2.8	1.6630	1.4093	1.1478	2.3436
2.9	1.5215	1.4037	1.0632	2.1357
3 (Case 1)	**1.4142**	**1.4142**	**1**	**2**
3.1	1.3290	1.4348	0.9503	1.9068
3.2	1.2589	1.4622	0.9099	1.8407
3.3	1.1997	1.4944	0.8760	1.7928
3.4	1.1488	1.5300	0.8470	1.7576
3.5 (Case 2)	**1.1042**	**1.5682**	**0.8217**	**1.7315**
3.6	1.0646	1.6084	0.7993	1.7123
3.7	1.0291	1.6502	0.7792	1.6982
3.8	0.9969	1.6932	0.7610	1.6880
3.9	0.9676	1.7372	0.7443	1.6809
4	0.9407	1.7820	0.7290	1.6762
4.1	0.9157	1.8274	0.7148	1.6735
4.2	0.8926	1.8734	0.7015	1.6722
4.3	0.8710	1.9198	0.6890	1.6721
4.4	0.8508	1.9666	0.6773	1.6731
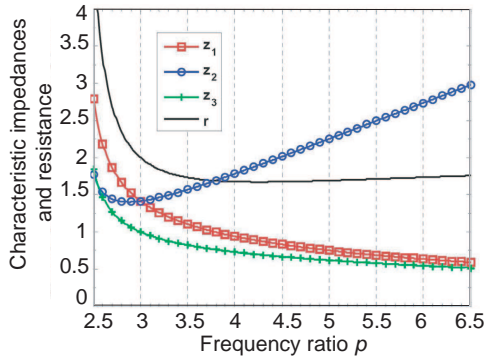
Figure 4. Normalized characteristic impedances and isolation resistance vs. frequency ratio p.

**Table 2.** Normalized design parameters with typical frequency ratios $(4.5 \leq p \leq 6.5)$.

The Frequency Ratio	Characteristic Impedances			Isolation Resistance
p	z_1	z_2	z_3	r
4.5	0.8317	2.0137	0.6661	1.6748
4.6	0.8137	2.061	0.6556	1.6772
4.7	0.7968	2.1086	0.6455	1.6800
4.8	0.7806	2.1563	0.6358	1.6833
4.9	0.7653	2.2042	0.6266	1.6869
5	0.7507	2.2522	0.6178	1.6908
5.1	0.7368	2.3003	0.6092	1.6949
5.2	0.7235	2.3485	0.6010	1.6991
5.3	0.7108	2.3967	0.5931	1.7035
5.4	0.6985	2.4450	0.5854	1.7079
5.5	0.6868	2.4933	0.5780	1.7124
5.6	0.6755	2.5416	0.5708	1.7169
5.7	0.6646	2.5900	0.5638	1.7214
5.8	0.6542	2.6384	0.5571	1.7259
5.9	0.6441	2.6867	0.5505	1.7305
6	0.6343	2.7351	0.5441	1.7349
6.1	0.6249	2.7835	0.5378	1.7394
6.2	0.6158	2.8319	0.5317	1.7438
6.3	0.6069	2.8802	0.5258	1.7481
6.4	0.5984	2.9286	0.5200	1.7524
6.5 (Case 3)	0.5901	2.9769	0.5143	1.7567

presented in Fig. 4, Table 1 and Table 2. When the frequency ratio is close to 6.5, the size of this power divider will very small, which is, the proposed structure has the function of miniaturization. It is interesting that the **Case 1** marked in Table 1 is the same with the conventional Wilkinson power divider [17].
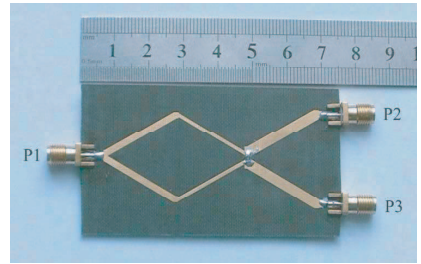
4. SIMULATION AND MEASUREMENT

To begin, a simulated dual-band power divider with high frequency ratio **(Case 3)** is presented according to the normalized design parameters given in Table 2. The operating frequencies are defined as 900 MHz and 5.85 GHz. This case belongs to examples of two high-separated bands. Based on ideal transmission line models, the final frequency responses are obtained and the absolute values of S-parameters are shown in Fig. 5. Obviously, the frequency responses agree well with the theoretical values (such as -3 dB in transmission parameters at center frequencies).

To certify this structure and the design parameters in experiment, the characteristic impedance of ports $Z_0 = 50\,\Omega$ is defined and a microstrip power divider operating at 1 GHz and 3.5 GHz ($p = 3.5$) is designed. From the results of Table 1 **(Case 2)**, the following design parameters can be obtained: $Z_1 = 1.1042 \times 50 = 55.210\,\Omega$, $Z_2 = 1.5682 \times 50 = 78.410\,\Omega$, $Z_3 = 0.8217 \times 50 = 41.085\,\Omega$, $R = 1.7315 \times 50 = 86.575\,\Omega$. The electrical length of all transmission lines at 1 GHz equals to $\pi/4.5$. The F4B substrate with 0.8-mm thickness and the dielectric constant of 2.65 is employed to fabricate
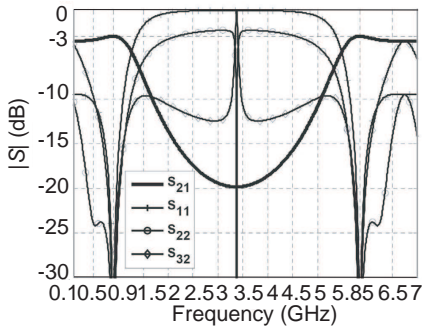
Figure 5. The frequency responses of a simulated power divider operating at both 900 MHz and 5.85 GHz.

Figure 6. The photograph of the fabricated power divider operating at 1 GHz and 3.5 GHz.
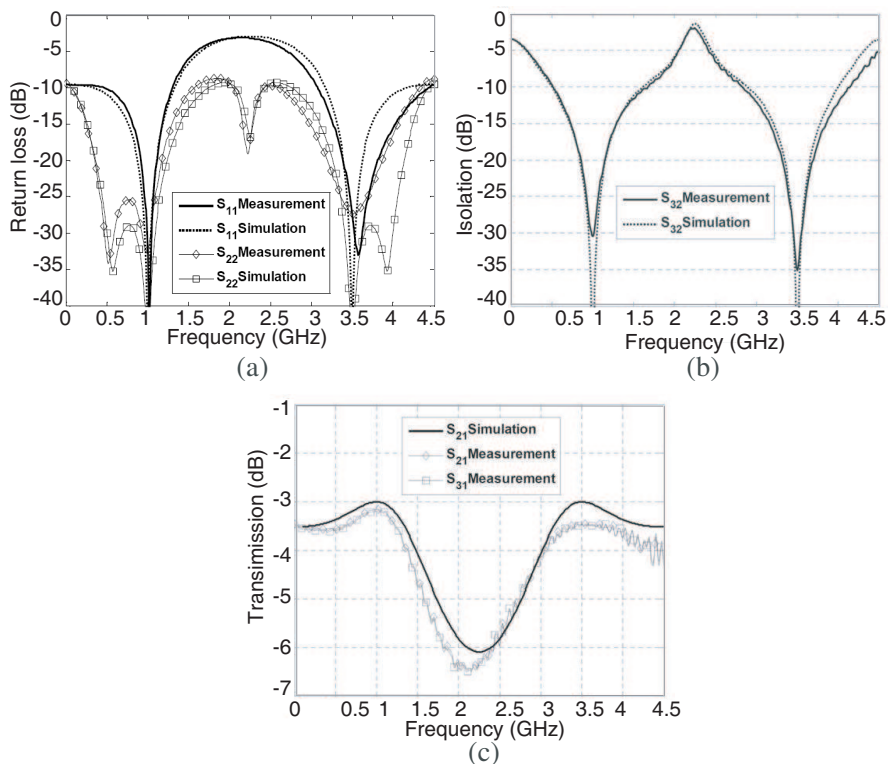
Figure 7. S-parameters of the fabricated power divider operating at both 1 GHz and 3.5 GHz. (a) Return loss (Simulation: $|S_{22}| = |S_{33}|$; Measurement: $|S_{22}| \cong |S_{33}|$). (b) Isolation (Simulation: $|S_{32}| = |S_{23}|$; Measurement: $|S_{32}| \cong |S_{23}|$). (c) Transmission (Simulation: $|S_{21}| = |S_{31}|$; Measurement: $|S_{21}| \cong |S_{31}|$).

this power divider, and the final photograph of the fabricated power divider with size $75 \times 43 \, \text{mm}^2$ is shown in Fig. 6. The simulated (based on ideal transmission line and resistor models) and measured (carried out by Agilent N5230C vector network analyzer) results are shown in Fig. 7. Obviously, there are good agreements between simulation and measurement. $|S_{11}|$, $|S_{22}|$, and $|S_{32}|$ are below $-25 \, \text{dB}$ at both 1 GHz and 3.5 GHz, while the insertion loss is $-3.18 \, \text{dB} \pm 0.3 \, \text{dB}$ at 1 GHz and $-3.47 \, \text{dB} \pm 0.3 \, \text{dB}$ at 3.5 GHz. In general, the performance shown in Fig. 7 indicates that the equal power dividing, the impedance matching at all ports and a good isolation between two output ports can be fulfilled at both 1 GHz and 3.5 GHz simultaneously. The lower value of insertion loss at 3.5 GHz (shown in Fig. 7(c)) may be caused

by high-frequency losses of F4B substrate and junction discontinuities in printed circuit board with SMA connectors. Measured bandwidths of 200 MHz at each band are found under the condition that isolation and matching are better than $-20\,$dB.

5. CONCLUSION

A novel modified Wilkinson power divider without transmission line stubs and reactive components for dual-band applications has been proposed, designed, and implemented in this paper. The design equations have been obtained by using rigorous even- and odd-mode analysis, and the normalized design parameters are given in both figure and table. A simulated dual-band example with high frequency ratio ($p = 6.5$) is presented to achieve theoretical verification. Furthermore, the simulated and measured results of a practical microstrip power divider indicate that it can operate at desired dual-band with good performances in return loss, equal power dividing and isolation. Actually, this proposed power divider is very suitable for the microstrip circuit implementation in dual-band wireless systems, in particular, the dual high-separated band communication systems.

REFERENCES

1. Monzon, C., "A small dual-frequency transformer in two sections," *IEEE Trans. Microw. Theory Tech.*, Vol. 51, No. 4, 1157–1161, 2003.
2. Wu, Y., Y. Liu, and S. Li, "A compact Pi-structure dual band transformer," *Progress In Electromagnetics Research*, PIER 88, 121–134, 2008.
3. Wu, Y., Y. Liu, and S. Li, "A dual-frequency transformer for complex impedances with two unequal sections," *IEEE Microw. Wireless Compon. Lett.*, Vol. 19, No. 2, 77–79, 2009.
4. Wu, L., Z. Sun, H. Yilmaz, and M. Berroth, "A dual-frequency Wilkinson power divider," *IEEE Trans. Microw. Theory Tech.*, Vol. 54, No. 1, 278–284, 2006.

5. Cheng, K. K. M. and F. L. Wong, "A new Wilkinson power divider design for dual band application," *IEEE Microw. Wireless Compon. Lett.*, Vol. 17, No. 9, 664–666, 2007.

6. Cheng, K.-K. M. and C. Law, "A novel approach to the design and implementation of dual-band power divider," *IEEE Trans. Microw. Theory Tech.*, Vol. 56, No. 2, 487–492, 2008.

7. Kawai, T., Y. Nakashima, Y. Kokubo, and I. Ohta, "Dual-band Wilkinson power dividers using a series RLC circuit," *IEICE Trans. Electron.*, Vol. E91-C, No. 11, 1793–1797, 2008.

8. Park, M. J. and B. Lee, "A dual-band Wilkinson power divider," *IEEE Microw. Wireless Compon. Lett.*, Vol. 18, No. 2, 85–87, 2008.

9. Park, M. J. and B. Lee, "Wilkinson power divider with extended ports for dual-band operation," *Electronics Letters*, Vol. 44, No. 15, 916–917, 2008.

10. Wu, Y., Y. Liu, and X. Liu, "Dual-frequency power divider with isolation stubs," *Electronics Letters*, Vol. 44, No. 24, 1407–1408, 2008.

11. Wu, Y., Y. Liu, and S. Li, "A new dual-frequency Wilkinson power divider," *Journal of Electromagnetic Waves and Applications*, Vol. 23, No. 4, 483–492, 2009.

12. Li, X., S.-X. Gong, L. Yang, and Y.-J. Yang, "A novel wilkinson power divider for dual-band operation," *Journal of Electromagnetic Waves and Applications*, Vol. 23, No. 2–3, 395–404, 2009.

13. Wu, Y., H. Zhou, Y. Zhang, and Y. Liu, "An unequal Wilkinson power divider for a frequency and its first harmonic," *IEEE Microw. Wireless Compon. Lett.*, Vol. 18, No. 11, 737–739, 2008.

14. Wu, Y., Y. Liu, Y. Zhang, J. Gao, and H. Zhou, "A dual band unequal wilkinson power divider without reactive components," *IEEE Trans. Microw. Theory Tech.*, Vol. 57, No. 1, 216–222, 2009.

15. Wu, Y., Y. Liu, and S. Li, "An unequal dual-frequency wilkinson power divider with optional isolation structure," *Progress In Electromagnetics Research*, PIER 91, 393–411, 2009.

16. Wu, Y., Y. Liu, and S. Li, "Unequal dual-frequency Wilkinson power divider including series resistor-inductor-capacitor isolation structure," *IET Microwaves, Antennas & Propagation*, Vol. 3, in press, 2009.

17. Wilkinson, E., "An N-way hybrid power divider," *IRE Trans. Microw. Theory Tech.*, Vol. 8, No. 1, 116–118, 1960.

18. Wu, Y. and Y. Liu, "Closed-form design method for unequal

lumped-elements Wilkinson power dividers," *Microwave and Optical Technology Letters*, Vol. 51, No. 5, 1320–1324, 2009.

19. Fan, F., Z.-H. Yan, and J.-B. Jiang, "Design of a novel compact power divider with harmonic suppression," *Progress In Electromagnetics Research Letters*, Vol. 5, 151–157, 2008.

20. Shamsinejad, S., M. Soleimani, and N. Komjani, "Novel miniaturized wilkinson power divider for 3 G mobile receivers," *Progress In Electromagnetics Research Letters*, Vol. 3, 9–16, 2008.

21. Oraizi, H. and M. S. Esfahlan, "Miniaturization of Wilkinson power dividers by using defected ground structures," *Progress In Electromagnetics Research Letters*, Vol. 4, 113–120, 2008.

22. Chang, C.-P., C.-C. Su, S.-H. Hung, Y.-H. Wang, and J.-H. Chen, "A 6 : 1 unequal wilkinson power divider with EBG CPW," *Progress In Electromagnetics Research Letters*, Vol. 8, 151–159, 2009.